Turning on and off the Rotational Oscillation of a Single Porphine Molecule by Molecular Charge State

Shichao Yan,[†] Zijing Ding,[†] Nan Xie,[†,‡] Huiqi Gong,[†] Qian Sun,[‡] Yang Guo,[†] Xinyan Shan,[†] Sheng Meng,[†,*] and Xinghua Lu[†,*]

[†]Beijing National Laboratory for Condensed-Matter Physics and Institute of Physics, Chinese Academy of Sciences, Beijing 100190, China and [‡]Photonics Center, College of Physics Science, Nankai University, Tianjin 300071, China

ABSTRACT

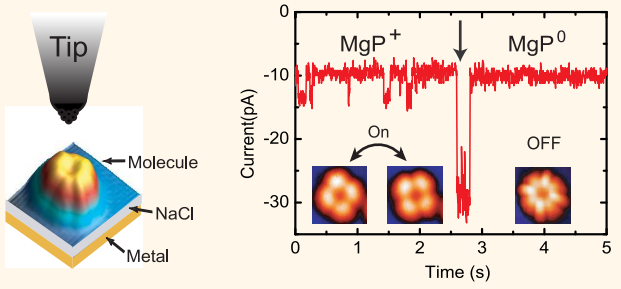

The rotation dynamics of single magnesium porphine molecules on an ultrathin NaCl bilayer is investigated with low-temperature scanning tunneling microscopy and density functional theory calculations. It is observed that the rotational oscillation between two stable orientations can be turned on and off by the molecular charge state, which can be manipulated with the tunneling electrons. The features of the charge states and the mechanism of molecular rotational on/off state control are revealed at the atomic scale. The dependence of molecular orientation switching rate on the tunneling electron energy and the current density illustrates the underlying resonant tunneling excitation and single-electron process. The drive and control of molecular motion with tunneling electrons demonstrated in this study suggests a novel approach toward electronically controlled molecular rotors and motors.

KEYWORDS: rotational oscillation · molecular charge state · NaCl bilayer · magnesium porphine · scanning tunneling microscopy · density functional theory

Observing and controlling rotational motion of a single molecule are essential for the development of nanoscale machines.[1] Significant progress has been made in observing rotational motion of individual molecules driven by light,[2,3] chemical reactions,[4,5] and electric current.[6−9] However, it still remains a great challenge to precisely manipulate the rotation direction,[9,10] speed,[11] and on/off states[12] at the single-molecule level. As a prospective candidate in building anchored molecular rotors and motors on a surface, metal porphine molecules and their derivatives are unique in their symmetric planar structure with a central metal atom.[13] Various dynamic behaviors in such molecules have been observed by scanning tunneling microscopy (STM) at the single-molecule level.[14−17] On the other hand, special attention has been focused on the characterization and the manipulation of their charge states.[14,18−20] However, the relationship between the rotational behavior of such molecules and their charge states has not been reported so far.

In this article, we report that the molecular charge state can be employed to turn on and off the rotational oscillation of a single magnesium porphine (MgP) molecule on an ultrathin insulating NaCl bilayer, as investigated with low-temperature STM and density functional theory (DFT) calculations. The positively charged molecular state enables rotational oscillation between two stable orientations driven by resonant tunneling electrons, while in the neutral state the rotational motion is strongly prohibited. An ultrathin NaCl bilayer is fabricated in our study to reduce the coupling between molecules and the metal substrate, so that the electronic excitation and the charge state manipulation can be achieved.

RESULTS AND DISCUSSION

Rectangular NaCl bilayer islands and individual MgP molecules are clearly resolved in STM images (Figure 1a). Molecules adsorbed on the bare metal surface appear as simple protrusions with no internal feature, as shown in the inset of Figure 1b. For molecules adsorbed on the NaCl bilayer, however, two significantly different molecular features were observed in high-resolution STM images (Figure 1b) by tunneling through the highest occupied molecular

* Address correspondence to smeng@aphy.iphy.ac.cn; xhlu@aphy.iphy.ac.cn.

Received for review February 7, 2012 and accepted April 2, 2012.

Published online April 02, 2012
10.1021/nn301099m

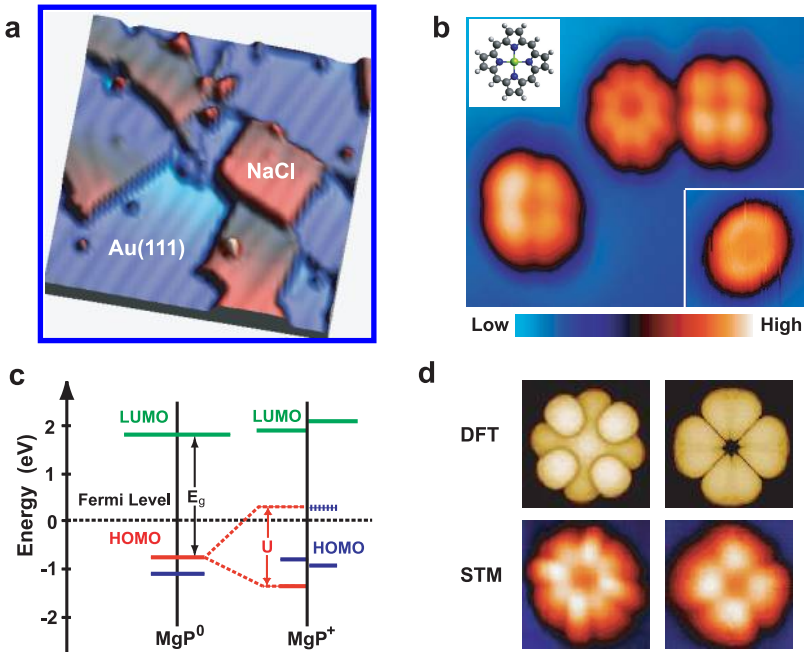

Figure 1. Two charge states of MgP molecules. (a) Constant current topographic image of MgP on Au(111) and NaCl islands at 10 K. The image size is 48 nm × 48 nm, taken at $V_b = -2.0$ V, $I = 10$ pA. (b) High-resolution topographic image of MgP molecules on the NaCl bilayer. The image size is 5.8 nm × 5.0 nm, taken at $V_b = -1.55$ V, $I = 1$ pA. The inset shows the image of MgP adsorbed on the Au(111) surface (2.1 nm × 2.1 nm, taken at $V_b = -1.25$ V, $I = 10$ pA) and the molecular structure of MgP. (c) Energy level diagram for neutral (MgP^0) and positively charged (MgP^+) molecules absorbed onto the NaCl/Au(111) surface. (d) Simulated images (top) from HOMO orbitals for both cases, as compared with experimentally measured STM images (bottom); the image size is 2.1 nm × 2.1 nm, taken at $V_b = -1.25$ V, $I = 1$ pA.

orbital (HOMO). These molecules on the NaCl bilayer can be classified as molecules with eight lobes (M8) and molecules with four lobes (M4). The population ratio of M8 to M4 molecules is about four to one, implying that M8 molecules are statistically more energy favorable.

The observed M4 and M8 configurations are two different charge states of the molecule, as revealed by first-principles calculations. Figure 1c presents a schematic diagram of the calculated electronic structure of a neutral and a positively charged MgP molecule adsorbed on the NaCl bilayer. For neutral molecules, the spin-degenerate HOMO and HOMO−1 orbitals are close in energy (orbital energy difference ~0.25 eV), and two degenerate lowest unoccupied molecular orbitals (LUMO) are located ~3 eV above.[21,22] For positively charged molecules, the original HOMO state splits into a singly unoccupied molecular orbital (SUMO) and a singly occupied molecular orbital (SOMO), due to onsite Coulomb repulsion. The splitting is so significant that the SOMO state is lower than the original HOMO−1 state, resulting in a swap of HOMO and HOMO−1. Simulated STM images of neutral MgP^0 and positively charged MgP^+ molecules resemble very well the M8 and M4 configurations observed in the experiment (Figure 1d). Thus, the combined STM images and first-principles calculations safely assign the M8 configuration to a neutral MgP^0 molecule and M4 to a positively charged MgP^+ molecule.

The rotational behavior of the molecule differs significantly in neutral and positively charged states. Excited by tunneling electrons, positively charged MgP^+ molecules oscillate between two stable orientations, while neutral MgP^0 molecules remain stable in the fixed orientation. The rotational oscillation of an MgP^+ molecule can be monitored through the tunneling current with the feedback turned off (Figure 2a). The low and high current levels represent two different orientations of the molecule. Figure 2b shows the STM images of a positively charged molecule in both orientations, in which the STM tip position is marked with star symbols. The rotational motion of the positively charged molecule can even be observed during STM scanning (see Figure S1 of the Supporting Information). In striking contrast, neutral molecules are stable in orientation and lateral displacements are usually induced at high enough current before observation of any rotational motion.

To understand the nature of tunneling electron induced rotational oscillation in positively charged molecules, we measured the orientation switching rate as a function of the STM sample bias. The switching rate is obtained with a standard exponential fit (see Figure S2 of the Supporting Information). Figure 2c shows a typical curve measured at the current set point of 10 pA, where the local density of states of the positively charged molecule is also presented for comparison (see Figure S3 of the Supporting Information). When the sample bias is set in the gap state region, the switching rate is almost zero, and it dramatically increases as the sample bias approaches

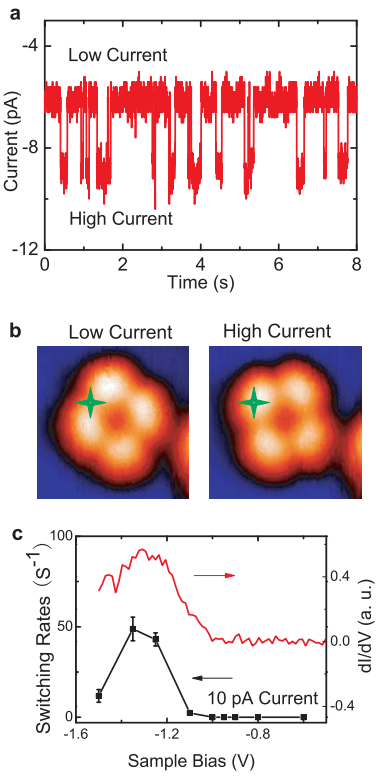

Figure 2. Rotational oscillation of a positively charged molecule. (a) Tunneling current *versus* time recorded. (b) STM images for a positively charged porphine molecule before and after rotation. The star marks the position of the STM tip for data collection. The image size is 2.4 nm × 2.4 nm, taken at $V_b = -1.7$ V, $I = 10$ pA. (c) Orientation switching rate as a function of sample bias when tunneling current is fixed at 10 pA.

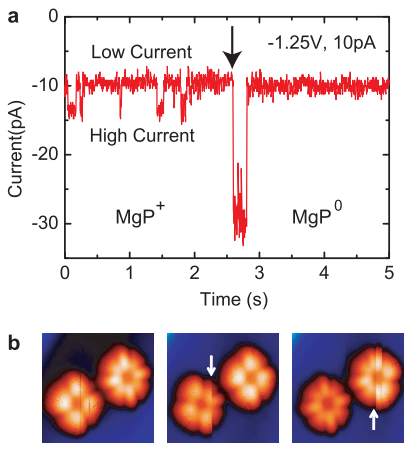

Figure 3. Controlling the rotational oscillation by molecular charge state and manipulation of molecular charge state. (a) Tunneling current *versus* time recorded during manipulation from the positively charged state to the neutral state. The transition is characterized by the big current pulse at $t = 2.5$ s and is confirmed by the scan thereafter. The arrow indicates the transition moment. (b) Sequence of STM images show molecular charge state transitions induced by the scanning tip. Arrows indicate the transitions during the scanning. The image size is 3.8 nm × 3.6 nm, taken at $V_b = -1.25$ V, $I = 1$ pA. The slow scan direction is from left to right.

the HOMO energy. The correlation between the threshold energy and the onset of the HOMO state illustrates that the observed molecular rotational motion is a resonant electronic excitation process.[8] We also find that the measured current switching rate rises linearly with the tunneling current set point, in the range between 1 and 10 pA, which is consistent with a statistically independent one-electron-induced molecular motion.[7]

The rotational behavior of the molecule can be determined by the charge state of the molecule, which can be manipulated with the tunneling electrons. Figure 3a shows a typical current *versus* time curve, which demonstrates the transition of a single molecule from oscillating state to stationary state. Under the tunneling electron excitation, the positively charged molecule first actively oscillates between two stable orientations, as revealed by the fluctuating current level in the initial two seconds. The molecule then switches into the neutral state with no current fluctuation, and the transition was captured as a big current pulse, which is indicated by the black arrow in Figure 3a. Manipulation from neutral state to positively charged state is also possible, but the yield is much lower than that for the opposite transition, probably due to the higher energy in the positively charged state. The feasibility of manipulation between neutral and positively charged states can also be seen during the STM scanning. Figure 3b shows a sequence of STM images of two molecules in the same area, acquired from left to right. As indicated by the arrows in the images, molecular charge state transitions in both directions are clearly captured during scanning. There is no lateral displacement during the charge state transitions, which excludes the possibility that the M4−M8 transition is due to the difference in adsorption site (see Figure S5 of the Supporting Information).

The critical role of molecular charge state in controlling rotation dynamics of a single MgP molecule can be understood at the atomic scale. Through atomic resolved STM images and extensive quantum mechanical calculations, the adsorption site and orientation of both neutral and positively charged molecules are precisely derived (Figure 4a, Figure S4 of the Supporting Information). The center of the molecule is positioned on top of Cl^- ions for both the neutral and positively charged molecules. Upon adsorption, the planar geometry of MgP is slightly distorted: the Mg atom is pulled downward from the molecular plane and the substrate Cl atom is pulled up by 0.3 Å. This results in a relatively strong Mg−Cl bond that serves as a shaft when the molecule rotates. Molecular orientation is defined by the angle θ between the Na−Cl bond and the Mg−N bond projected onto the NaCl surface. Figure 4b shows rotational potential energy surfaces for both neutral and positively charged molecules in the range of $-45° \leq \theta \leq 45°$. The most stable orientation is $\theta = \pm 25°$ for neutral molecules and $\theta = \pm 14°$ for

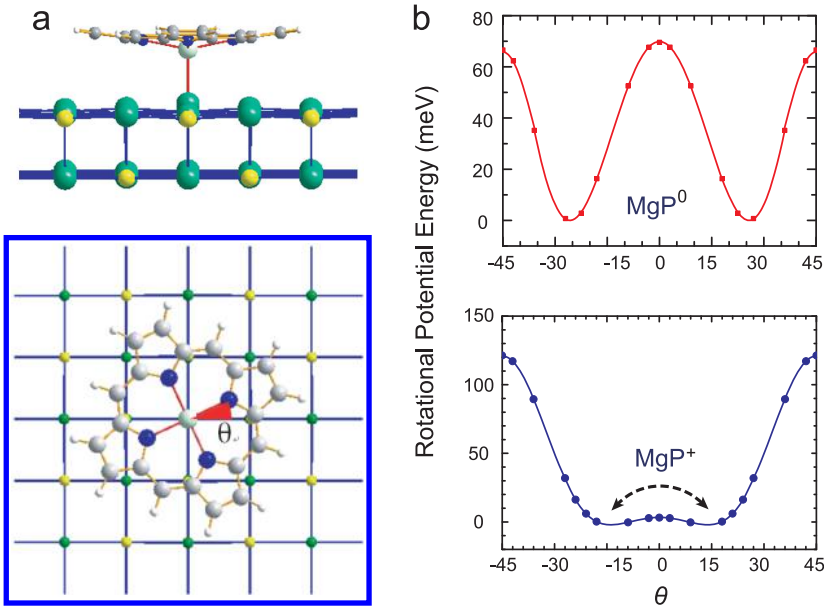

Figure 4. Adsorption configuration and rotational potential energy. (a) Side and top view of optimized geometry of MgP adsorption on NaCl bilayer. (b) Rotational potential energy as a function of angle θ for neutral MgP^0 and charged MgP^+ molecules. The dashed arrow indicates the rotation between two orientations of a charged MgP^+ molecule.

positively charged molecules. The minimal potential energy barrier between two stable orientations is 70 meV for neutral molecules and 5 meV for positively charged molecules, which oscillate between two stable orientations. At low temperature, ~10 K (thermal energy ~0.9 meV), we thus expect much less rotation probability in neutral molecules than in positively charged molecules, which is consistent with our experimental observations. The potential energy barrier can be roughly understood as the result of the Coulomb interaction between ionic surface and molecular charge density. The dramatic change in potential energy barrier is thus due to the significant difference in spatial distribution of the molecular orbitals in different charge states. We also simulated STM images at the stable orientations for both neutral and charged molecules, which match well with the experimental observations.

The significance of this study is revealed by the feasibility in manipulating molecular charge states. Besides STM tunneling electrons, molecular charge states can also be manipulated with many other techniques, such as electric gate,[23,24] photon excitation,[25] and chemical reactions. In principle, the control mechanism demonstrated in our STM experiments can be applied to these situations as well. Especially, the insulating NaCl bilayer used in our study illustrates the prospect of constructing a charge state controlled molecular rotor in a gated single-molecule transistor configuration. In addition, porphine molecules are of special interest in photon energy conversion, molecular electronics, and supramolecular design.[13] The illustrated static property and charge-state-dependent dynamic processes of MgP molecules are valuable to the related applications.

CONCLUSIONS

In summary, we have revealed a novel mechanism in manipulating rotational oscillation of a single molecule through its charge state. The rotational oscillation can be turned on and off simply by tuning the molecule into positively charged or neutral molecular states. The combined STM study and first-principles calculations provide insight into the control mechanism at the atomic scale, as well as the nature of the resonant tunneling induced rotation dynamics of a single-molecule switch. The underlying mechanism revealed in this study illustrates a novel approach toward reversibly controlled molecular rotors and motors by manipulating its charge states, which can be implemented by various techniques including microfabricated electric gates.

EXPERIMENTAL SECTION

Our experiments were conducted using a home-built ultra-high-vacuum STM operated at 10 K.[26] The Au(111) single-crystal substrate was cleaned by cycles of Ar^+ ion sputtering and annealing to 900 K. Atomic-flat NaCl islands were prepared by thermally evaporating NaCl at 650 K onto a Au(111) substrate surface, which was held at room temperature. MgP molecules were thermally evaporated onto the sample surface after the substrate was cooled to 10 K. Chemically etched Ag wire was used as the STM tip in this study. To measure the electronic local density of states, the d*I*/d*V* signal was recorded with the lock-in technique under the open-loop conditions. The bias

modulation was 10 mV (rms) at 361.1 Hz (the bias voltages here refer to the sample bias with respect to the tip). The WSxM program (www.nanotec.es) was used to display the STM images.

The first-principles calculations were carried out within the framework of density functional theory, employing PAW pseudopotentials[27,28] and the PBE form[29] of the exchange–correlation functional, as implemented in VASP code.[30] The experimental NaCl lattice constant of 5.64 Å and ($3\sqrt{2}\times3\sqrt{2}$) surface unit cell (36 atoms per layer) is used to model the NaCl bilayer substrate.[31] We employ an energy cutoff of 400 eV for plane waves, and the criterion for total energy convergence is set to 10^{-4} eV. STM images were simulated from a spatial distribution of HOMO electrons based on the Tersoff–Hamann approximation.[32] Mixing of nearly degenerate HOMO states was used to mimic the effect of substrate on STM images. The HOMO is set to ~1 eV below the Fermi level of Au(111) (dotted black line), inferred from measured STS data.

Conflict of Interest: The authors declare no competing financial interest.

Acknowledgment. This work has been supported by the National Basic Research Program of China (Grant Nos. 2012CB933002, 2012CB921403), the Natural Science Foundation of China (Grants Nos. 10974245, 11174347, 11074287), and Chinese Academy of Sciences (Grant No. 07C3021B51, Hundred-Talent Project).

Supporting Information Available: (1) Molecular rotational motion captured during STM scanning; (2) measuring molecular switching rate; (3) molecular local density of states; (4) molecular adsorption site and orientation; (5) lateral displacement check between 4-lobe and 8-lobe configurations. This material is available free of charge *via* the Internet at http://pubs.acs.org.

REFERENCES AND NOTES

1. Browne, W. R.; Feringa, B. L. Making Molecular Machines Work. *Nat. Nanotechnol.* **2006**, *1*, 25–35.
2. Koumura, N.; Zijlstra, R. W. J.; van Delden, R. A.; Harada, N.; Feringa, B. L. Light-Driven Monodirectional Molecular Rotor. *Nature* **1999**, *401*, 152–155.
3. van Delden, R. A.; ter Wiel, M. K. J.; Pollard, M. M.; Vicario, J.; Koumura, N.; Feringa, B. L. Unidirectional Molecular Motor on a Gold Surface. *Nature* **2005**, *437*, 1337–1340.
4. Kelly, T. R.; Silva, R. A.; De Silva, H.; Jasmin, S.; Zhao, Y. J. A Rationally Designed Prototype of a Molecular Motor. *J. Am. Chem. Soc.* **2000**, *122*, 6935–6949.
5. Leigh, D. A.; Wong, J. K. Y.; Dehez, F.; Zerbetto, F. Unidirectional Rotation in a Mechanically Interlocked Molecular Rotor. *Nature* **2003**, *424*, 174–179.
6. Gimzewski, J. K.; Joachim, C.; Schlittler, R. R.; Langlais, V.; Tang, H.; Johannsen, I. Rotation of a Single Molecule within a Supramolecular Bearing. *Science* **1998**, *281*, 531–533.
7. Stipe, B. C.; Rezaei, M. A.; Ho, W. Inducing and Viewing the Rotational Motion of a Single Molecule. *Science* **1998**, *279*, 1907–1909.
8. Lastapis, M.; Martin, M.; Riedel, D.; Hellner, L.; Comtet, G.; Dujardin, G. Picometer-Scale Electronic Control of Molecular Dynamics inside a Single Molecule. *Science* **2005**, *308*, 1000–1003.
9. Tierney, H. L.; Murphy, C. J.; Jewell, A. D.; Baber, A. E.; Iski, E. V.; Khodaverdian, H. Y.; McGuire, A. F.; Klebanov, N.; Sykes, E. C. H. Experimental Demonstration of a Single-Molecule Electric Motor. *Nat. Nanotechnol.* **2011**, *6*, 625–629.
10. Michl, J.; Sykes, E. C. H. Molecular Rotors and Motors: Recent Advances and Future Challenges. *ACS Nano* **2009**, *3*, 1042–1048.
11. Vicario, J.; Walko, M.; Meetsma, A.; Feringa, B. L. Fine Tuning of the Rotary Motion by Structural Modification in Light-Driven Unidirectional Molecular Motors. *J. Am. Chem. Soc.* **2006**, *128*, 5127–5135.
12. Kelly, T. R.; Bowyer, M. C.; Bhaskar, K. V.; Bebbington, D.; Garcia, A.; Lang, F. R.; Kim, M. H.; Jette, M. P. A Molecular Brake. *J. Am. Chem. Soc.* **1994**, *116*, 3657–3658.
13. Chou, J. H.; Kosal, M. E.; Nalwa, H. S.; Rakow, N. A.; Suslick, K. S. Applications of Porphyrins and Metalloporphyrins to Materials Chemistry. In *The Porphyrin Handbook*; Kadish, K. M., Smith, K. M., Guilard, R., Eds.; Academic Press: New York, 2000; pp 44–67.
14. Wu, S. W.; Ogawa, N.; Ho, W. Atomic-Scale Coupling of Photons to Single-Molecule Junctions. *Science* **2006**, *312*, 1362–1365.
15. Chen, C.; Chu, P.; Bobisch, C. A.; Mills, D. L.; Ho, W. Viewing the Interior of a Single Molecule: Vibronically Resolved Photon Imaging at Submolecular Resolution. *Phys. Rev. Lett.* **2010**, *105*, 217402.
16. Qiu, X. H.; Nazin, G. V.; Ho, W. Vibrationally Resolved Fluorescence Excited with Submolecular Precision. *Science* **2003**, *299*, 542–546.
17. Auwaerter, W.; Seufert, K.; Bischoff, F.; Ecija, D.; Vijayaraghavan, S.; Joshi, S.; Klappenberger, F.; Samudrala, N.; Barth, J. V. A Surface-Anchored Molecular Four-Level Conductance Switch Based on Single Proton Transfer. *Nat. Nanotechnol.* **2012**, *7*, 41–46.
18. Fu, Y.-S.; Zhang, T.; Ji, S.-H.; Chen, X.; Ma, X.-C.; Jia, J.-F.; Xue, Q.-K. Identifying Charge States of Molecules with Spin-Flip Spectroscopy. *Phys. Rev. Lett.* **2009**, *103*, 257202.
19. Swart, I.; Sonnleitner, T.; Repp, J. Charge State Control of Molecules Reveals Modification of the Tunneling Barrier with Intramolecular Contrast. *Nano Lett.* **2011**, *11*, 1580–1584.
20. Leoni, T.; Guillermet, O.; Walch, H.; Langlais, V.; Scheuermann, A.; Bonvoisin, J.; Gauthier, S. Controlling the Charge State of a Single Redox Molecular Switch. *Phys. Rev. Lett.* **2011**, *106*, 216103.
21. Seda, J.; Burda, J. V.; Leszczynski, J. Study of Electronic Spectra of Free-Base Porphin and Mg-Porphin: Comprehensive Comparison of Variety of Ab Initio, DFT, and Semiempirical Methods. *J. Comput. Chem.* **2005**, *26*, 294–303.
22. Maddox, J. B.; Harbola, U.; Mayoral, K.; Mukamel, S. Conductance Bistability in a Single Porphyrin Molecule in a STM Junction: A Many-Body Simulation Study. *J. Phys. Chem. C* **2007**, *111*, 9516–9521.
23. Park, H.; Park, J.; Lim, A. K. L.; Anderson, E. H.; Alivisatos, A. P.; McEuen, P. L. Nanomechanical Oscillations in a Single-C-60 Transistor. *Nature* **2000**, *407*, 57–60.
24. Liang, W. J.; Shores, M. P.; Bockrath, M.; Long, J. R.; Park, H. Kondo Resonance in a Single-Molecule Transistor. *Nature* **2002**, *417*, 725–729.
25. Sariciftci, N. S.; Smilowitz, L.; Heeger, A. J.; Wudl, F. Photoinduced Electron-Transfer from a Conducting Polymer to Buckminsterfullerene. *Science* **1992**, *258*, 1474–1476.
26. Stipe, B. C.; Rezaei, M. A.; Ho, W. A Variable-Temperature Scanning Tunneling Microscope Capable of Single-Molecule Vibrational Spectroscopy. *Rev. Sci. Instrum.* **1999**, *70*, 137–143.
27. Vanderbilt, D. Soft Self-Consistent Pseudopotentials in a Generalized Eigenvalue Formalism. *Phys. Rev. B* **1990**, *41*, 7892–7895.
28. Blöchl, P. E. Projector Augmented-Wave Method. *Phys. Rev. B* **1994**, *50*, 17953–17979.
29. Perdew, J. P.; Burke, K.; Ernzerhof, M. Generalized Gradient Approximation Made Simple. *Phys. Rev. Lett.* **1996**, *77*, 3865–3868.
30. Kresse, G.; Hafner, J. Ab Initio Molecular Dynamics for Liquid Metals. *Phys. Rev. B* **1993**, *47*, 558–561.
31. The effect of a Au(111) surface and its reconstruction on molecular adsorption is complicated, but it is expected to serve mainly as an electron reservoir during tunneling experiments; therefore, we eliminate the gold surface from our model and employ a NaCl bilayer as the substrate to make the computation affordable.
32. Tersoff, J.; Hamann, D. R. Theory of the Scanning Tunneling Microscope. *Phys. Rev. B* **1985**, *31*, 805–813.